Neutron-scattering study of the nuclear and magnetic structure of DyD_3 and associated vibrational and magnetic excitations

T. J. Udovic, Q. Huang,* J. W. Lynn, R. W. Erwin, and J. J. Rush
NIST Center for Neutron Research, National Institute of Standards and Technology, Gaithersburg, Maryland 20899
(Received 12 August 1998)

Neutron-diffraction and inelastic-scattering measurements of the hexagonal rare-earth trideuteride DyD_3 were undertaken between 1.27 and 295 K. Rietveld-refined, $P\bar{3}c1$-symmetric models of the diffraction data as well as the observed neutron vibrational spectra indicate that DyD_3 is crystallographically isostructural with YD_3 and HoD_3 over the temperature range measured. Below $T_N = 3.33(4)$ K, the Dy sublattice becomes antiferromagnetically ordered, with the $5.25(4)\mu_B$ moment along the c direction. In addition, the first crystal-field excitation for the $J = 15/2$ Dy ion has been identified at 7.79(8) meV. [S0163-1829(99)02318-8]

INTRODUCTION

Besides their interesting optical properties,[1,2] the hexagonal trihydrides of a number of the heavier rare-earth metals, namely, Gd,[3] Dy,[4] and Er,[5] were found by magnetic-susceptibility measurements to undergo an antiferromagnetic ordering transition at low temperature, with ordering temperatures of 1.8, 3.2, and 0.6 K, respectively. To the best of our knowledge, no neutron-scattering-based magnetic studies have been performed subsequent to these early works to ascertain the details of the nuclear and magnetic structures and the related crystal-field excitations. Indeed, it appears that such studies concerning the magnetic behavior of the rare-earth hydrides have been largely limited to the cubic dihydride phases.[6] With this in mind, we undertook a neutron-scattering study to characterize the nuclear and magnetic configurations of DyD_3 as well as the associated vibrational and magnetic excitations.

DyD_3 forms by a first-order phase transition from the fcc β-phase DyD_{2+x} when x exceeds ~ 0.18.[7] (The corresponding phase boundary for DyH_{2+x} has been reported to occur at ~ 0.23.[8]) Vajda *et al.*[9] investigated the magnetic structures of β-DyD_{2+x} by neutron powder diffraction (NPD), improving on some earlier work by Shaked *et al.*[10] For $x = 0$, an incommensurate antiferromagnetic structure was observed below 5.0 K, which transformed with hysteresis into a nearly commensurate antiferromagnetic structure below ~ 2.5–3.5 K. For $x = 0.135$, no long-range magnetic order was observed. Rather, a single broad magnetic feature was suggestive of only short-range magnetic order below ~ 4–6 K. The linewidth was consistent with the presence of magnetic domains of ~ 30 Å.

The magnetic susceptibility of DyH_3 was found by Carlin and Krause[4] to pass through a broad maximum at 3.5 K followed by a substantial decrease upon a further lowering of the temperature, with the 3.2(1) K antiferromagnetic ordering temperature determined from the maximum value of the temperature derivative of the susceptibility. Earlier Mössbauer results[11] failed to observe the hyperfine structure anticipated from magnetic ordering of DyH_3, even at 1.6 K. Carlin and Krause[4] postulated that, since DyH_3 was an insulator, the magnetic hyperfine splitting was probably precluded by the sufficiently fast spin relaxation still present at this low temperature.

Typical of the other heavier rare-earth trihydride systems,[12,13] DyH_3 was found by x-ray diffraction to possess an hcp metal lattice. Although no NPD studies of DyD_3 have been reported, such studies of the related HoD_3 (Ref. 14) and YD_3 (Refs. 15–17) systems have indicated a single structure possessing $P\bar{3}c1$ (D_{3d}^4) symmetry. Figure 1 displays a schematic of the corresponding unit cell (see Table I for nuclear positions), which is a $(\sqrt{3}\times\sqrt{3})R30°$ expansion of the conventional hcp unit cell in the ab plane ($a = \sqrt{3}a_0$, $c = c_0$). To accommodate the D atoms, there is an increase in the c-axis separation between metal basal planes compared to the virgin hcp metal. The D atoms occupy unusual interstitial positions instead of the more conventional octahedral (o) and tetrahedral (t) sites. The D_o atoms are displaced vertically toward the metal planes (i.e., m sites) from their ideal o-site positions, with correlated siting at either in-plane ($m1$) or near-plane ($m2$) threefold positions. The presence of each D_{m1} atom causes a slight radial expansion of the three neighboring metal atoms, yielding lateral displacements from the high-symmetry positions. The D_{m2} atoms are divided evenly between sites slightly above and below the metal planes. The D_t atoms undergo correlated horizontal displacements with respect to the positions of the D_{m2} atoms. In particular, when a D_{m2} atom is vertically displaced above (below) the metal layer, the three nearest-neighbor D_t atoms in the D_t layer above (below) the metal layer move away from the vertical displacement axis, and the three nearest-neighbor D_t atoms in the D_t layer below (above) the metal layer move toward the vertical displacement axis. The contraction and expansion of the corresponding D_t triads are nonradial, occurring with significant horizontal twists.

In the most recent YD_3 study,[16] the assumption of full occupation of the $m1$ and $m2$ sites resulted in exceptionally large temperature factors for the D_m atoms along the c axis. This suggested that some partial disorder of the D_m atoms was occurring along this axis. The disorder appeared to involve c-axis displacements of some D_m atoms from in-metal-plane ($m1$) to near-plane ($m1'$) positions as well as from near-plane ($m2$) to in-plane ($m2'$) positions, such that the total m-site occupancies of the metal-plane and near-metal-

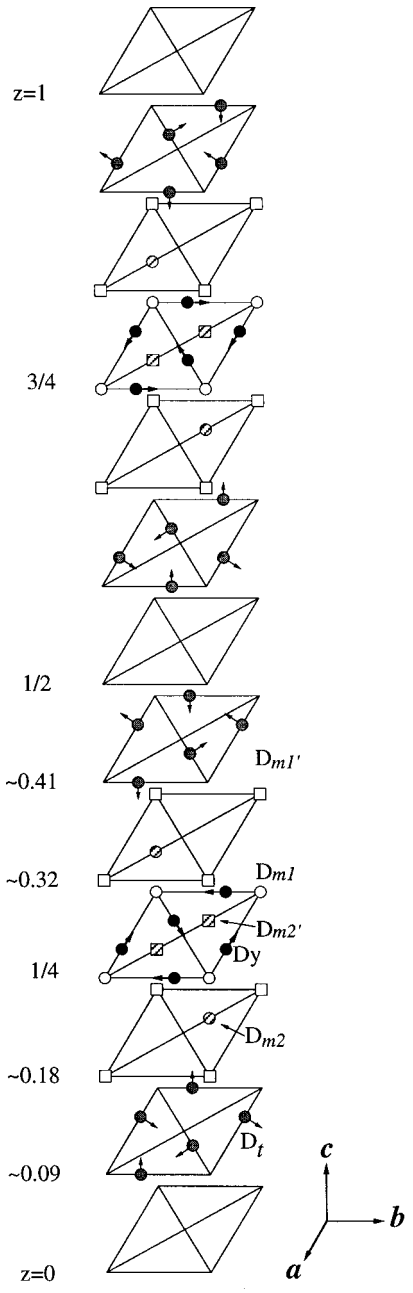

FIG. 1. Exploded view of the $P\bar{3}c1$ structural model previously determined for YD_3 (Ref. 16). Horizontal displacement vectors indicate the direction of the t and metal-site displacements. In the perfectly ordered structure, t, $m1$, and $m2$ sites are fully occupied while $m1'$ and $m2'$ sites are empty. In the proposed partially ordered structure, $m1'$ and $m2'$ sites are partially occupied with reduced occupation of $m1$ and $m2$ sites, as described in the text. The c-axis locations of the various layers are labeled with the values determined from the disorder-model refinement.

plane layers remained unchanged. This condition is fulfilled when the occupancies of the $m1'$ and $m2'$ disorder sites are equivalent. The occupancies of these sites, which would be zero for perfectly ordered YD_3, were found by model fits to range from ~13% at the lowest temperatures to ~18% at 400 K.

Theoretical calculations concerning the hcp rare-earth-trihydride structure have been the subject of some controversy in recent years. Wang and Chou[18,19] and Dekker *et al.*[20] corroborated the greater stability of the $P\bar{3}c1$ structure for YH_3 compared to the alternative fcc structure by first-principles, total-energy calculations. The drawback of these calculations was the prediction of metallic behavior for the $P\bar{3}c1$ structure. This seemed inconsistent with the optical and electrical measurements on YH_x by Huiberts *et al.*[1] which indicated that YH_3 was an insulator with a large band gap. Subsequently, Kelly *et al.*[21] suggested by similar calculations that a lower-energy, broken-symmetry ($P3$) insulating structure existed, more consistent with the measurements of Huiberts *et al.* Unfortunately, this structure appeared to be inconsistent with the NPD studies[16,17] for YD_3, which failed to observe the extra Bragg reflections that would accompany the lower symmetry. More recently, Ahuja *et al.*[22] have performed total-energy calculations for the higher-symmetry $P\bar{3}c1$ structure using an all-electron, full-potential, linear muffin-tin orbital technique and have indeed predicted an electronic structure with a small band gap. Finally, Eder *et al.*[23] have indicated that the prediction of a band gap in these materials results quite naturally from the inclusion of a charge-dependent radius for the H ion in the band-structure calculations.

EXPERIMENTAL PROCEDURE

Synthesis of the DyD_3 sample was accomplished by the following procedure. Approximately 5 g of high-purity Dy (Johnson Matthey, 99.99 at. % metal purity; with 50, 30, 20, and 1 ppm impurity levels for Cu, Al, Fe, and Mn, respectively) were slowly loaded with D_2 (Cambridge Isotope Laboratories 99.98% isotopic purity) by gas-phase absorption in a quartz tube at 873 K. After absorbing ~2 D/Dy (which is the maximum expected uptake at this temperature under the final vapor pressure of 80 kPa D_2) to form the cubic dideuteride, the temperature was lowered over 4 h to 455 K under a similar D_2 pressure. During this cool down, the sample absorbed additional D_2 to form the bulk of the final trideuteride. The sample was held at 455 K for 15 h under 53 kPa D_2, then cooled to room temperature (~295 K) over 1 h. After equilibration for an additional 4 h at room temperature, the D_2 was evacuated from the quartz tube and the tube was quickly placed inside a He-filled glovebox. The DyD_3 was removed from the quartz tube and pulverized using a mortar and pestle. Next, the finely powdered sample was placed within an Al foil pouch and reloaded into the quartz tube for a final treatment in 67 kPa D_2 at 473 K for 15 h, followed by a cool down to room temperature over 1.5 h. The final stoichiometric ratio as determined by quantitative volumetric uptake was 2.995(8) D/Dy, which is in line with the reported ratio for a similarly prepared sample.[4] After the D_2 was reevacuated from the quartz tube, the sample was unloaded once again in the glovebox and placed into a double-walled annular V container (50 mm ht.×12 mm outer diam. and 1 mm annular cavity thickness) for neutron-scattering measurements. The annular geometry was used to minimize the effects of the large neutron absorption cross section for Dy (850 b at 1.54 Å).[24] The V container was promptly sealed to minimize any slow room-temperature evolution of D_2. With this procedure, negligible D was lost before final isolation in the container. Moreover, due to the

TABLE I. Comparison of the $P\bar{3}c1$ nuclear parameters for DyD_3 and YD_3 (Ref. 16) using the perfect-order and partial-disorder models. [n and B refer to occupancy and temperature factor, respectively. Constraints for the disorder model are: $z(D_{m2'})=1/4$; $z(D_{m1'})=z(D_{m2})$; $n(D_{m2'})=n(D_{m1'})=1-n(D_{m2})$; $n(D_{m1})=1-2n(D_{m2'})$; $B(D_{m1})=B(D_{m1'})=B(D_{m2})=B(D_{m2'})$].

					Perfect-order model		Partial-disorder model		
Atom		Position		Parameter	(YD_3) 295 K	(DyD_3) 295 K	(YD_3) 295 K	(DyD_3) 295 K	(DyD_3) 1.27 K
				a(Å)	6.3440(2)	6.3442(2)	6.3440(2)	6.3443(2)	6.3281(1)
				c(Å)	6.5997(3)	6.5984(3)	6.5999(2)	6.5983(3)	6.5912(1)
				V(Å^3)	230.03(2)	230.00(2)	230.04(2)	230.01(2)	228.58(1)
R	$6f$	2.	(x,0,1/4)	x	0.6637(7)	0.6689(7)	0.6637(7)	0.6721(6)	0.6733(4)
(Y, Dy)				n	1	1	1	1	1
				B(Å^2)	0.34(2)	0.41(2)	0.38(2)	0.36(2)	0.23(2)
D_t	$12g$	1	(x,y,z)	x	0.3521(5)	0.346(1)	0.3526(5)	0.351(1)	0.3479(8)
				y	0.0321(3)	0.0328(9)	0.0317(3)	0.031(1)	0.027(1)
				z	0.0903(2)	0.0899(5)	0.0903(2)	0.0898(5)	0.0928(3)
				n	1	1	1	1	1
				B(Å^2)					
				B_{11}(Å^2)	1.9(1)	1.8(2)	2.11(9)	0.7(3)	0.7(1)
				B_{22}(Å^2)	1.9(1)	3.1(3)	1.65(9)	3.9(4)	4.0(3)
				B_{33}(Å^2)	1.13(4)	2.1(1)	1.11(4)	1.7(1)	1.06(6)
				B_{12}(Å^2)	1.4(1)	2.0(2)	1.23(8)	1.2(2)	1.2(1)
				B_{13}(Å^2)	0.1(1)	2.1(2)	0.1(1)	−0.4(2)	0.3(1)
				B_{23}(Å^2)	−0.06(5)	0.5(2)	−0.11(5)	0.2(2)	0.9(1)
D_{m1}	$2a$	32.	(0,0,1/4)	n	1	1	0.676(9)	0.57(4)	0.78(3)
				B(Å^2)			0.84(3)	0.93(7)	1.10(6)
				B_{11}(Å^2)	0.5(2)	0.0(4)			
				B_{22}(Å^2)	0.5(2)	0.0(4)			
				B_{33}(Å^2)	6.7(4)	16(3)			
				B_{12}(Å^2)	0.24(8)	0.0(2)			
$D_{m1'}$	$4c$	3..	(0,0,z)	z			0.1814(3)	0.1804(7)	0.1768(6)
				n			0.162(4)	0.22(2)	0.16(1)
				B(Å^2)			0.84(3)	0.93(7)	1.10(6)
D_{m2}	$4d$	3..	(1/3,2/3,z)	z	0.1874(6)	0.194(2)	0.1814(3)	0.1804(7)	0.1768(6)
				n	1	1	0.838(4)	0.78(2)	0.84(1)
				B(Å^2)			0.84(3)	0.93(7)	1.10(6)
				B_{11}(Å^2)	0.84(8)	1.2(2)			
				B_{22}(Å^2)	0.84(8)	1.2(2)			
				B_{33}(Å^2)	2.8(1)	3.2(4)			
				B_{12}(Å^2)	0.42(4)	0.6(1)			
$D_{m2'}$	$4d$	3..	(1/3,2/3,z)	z			1/4	1/4	1/4
				n			0.162(4)	0.22(2)	0.16(1)
				B(Å^2)			0.47(7)	0.93(7)	1.10(6)
				R_p(%)	4.66	4.02	4.38	4.05	3.36
				R_{wp}(%)	6.14	4.74	5.57	4.77	3.95
				χ^2	1.042	1.023	1.051	1.036	1.269

small sample dead volume, very little D was lost in order to establish the equilibrium D_2 vapor pressure in contact with the sealed sample, and no further effort was made to repressurize the container with D_2. During the experiments, the sample was mounted in a pumpable liquid-He, top-loading cryostat.

Similar procedures and H_2 (Matheson Research Grade) were used to synthesize a 5-g sample of DyH_3 for vibrational spectroscopic measurements. The sample was loaded into an Al flat-plate container and measurements were performed in a temperature-controlled, closed-cycle He refrigerator.

All experiments were performed at the Neutron Beam Split-Core Reactor within the NIST Center for Neutron Research. The NPD measurements were taken with the high-

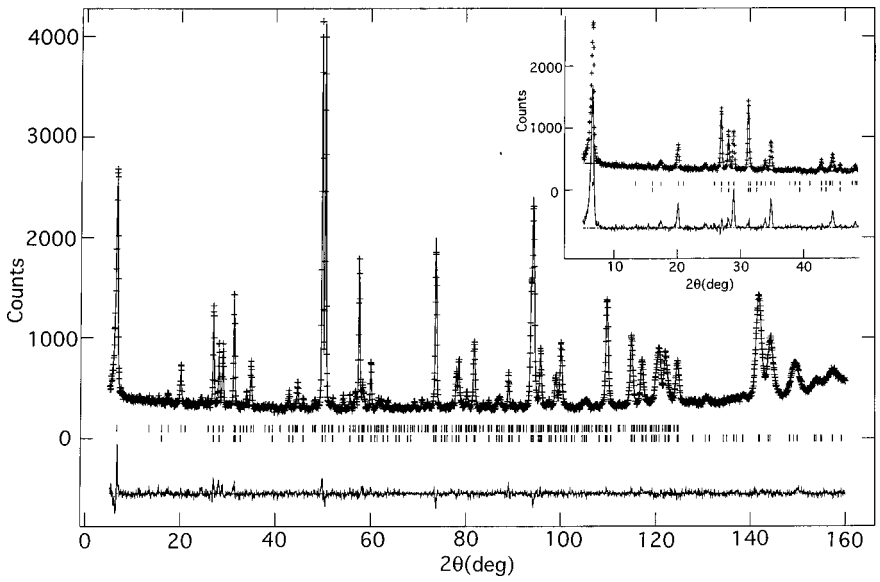

FIG. 2. NPD pattern for DyD_3 at 1.27 K and the corresponding fit (solid line) of the nuclear +magnetic structure. Below the data is the difference pattern between calculated and observed intensities as well as an upper and lower series of vertical lines to mark the calculated positions of the magnetic and nuclear Bragg reflections, respectively. Magnetic contributions are displayed by the low-angle region of the difference pattern in the inset, where the nuclear portion of the model fit is subtracted from the data. Details of the model fits are described in the text.

resolution, 32-counter BT-1 diffractometer.[25] The Cu(311) monochromator was used at a wavelength of 1.5401(1) Å. The wavelength was calibrated using a NIST Si standard reference material. The horizontal divergences were 15′, 20′, and 7′ of arc for the in-pile, monochromatic-beam, and diffracted-beam collimators, respectively. Data were collected every 0.05° over a 2θ angular range of 3 to 168°. All refinements were carried out with the Rietveld method[26] using the program GSAS.[27] Neutron-scattering amplitudes used in the refinements were 16.9 fm for Dy and 6.67 fm for D.[23] Wavelength errors were not included in the standard deviations of the unit cells, i.e., the precisions reported in this paper for the structural parameters reflect the quality of the data and the corresponding Rietveld refinement model, assuming a fixed neutron wavelength.

The temperature dependence of the magnetic ordering transition and crystal-field excitations were investigated using the BT-2 triple-axis spectrometer. For the diffraction data, the PG(002) monochromator was used at a wavelength of 2.35 Å with a PG filter. The horizontal divergences were 60, 40, 40, and 40 min of arc for the in-pile, monochromatic-beam, and diffracted-beam, and detector collimators, respectively. The magnetic inelastic data were collected with a fixed final energy of 14.7 meV.

The neutron vibrational spectra for DyD_3 and DyH_3 were measured with the BT-4 spectrometer using the low-resolution Be filter and high-resolution Be-graphite-Be-filter analyzers. The corresponding final energies were taken as 3.0 and 1.2 meV, respectively. The horizontal divergences for the in-pile and monochromatic-beam collimators were both 20 min of arc for the low-resolution configuration and 40 min for the high-resolution configuration. The full-width-at-half-maximum (FWHM) instrumental resolution is displayed with the spectra.

RESULTS AND DISCUSSION

Figure 2 illustrates the DyD_3 powder pattern measured at 1.27 K, and the corresponding fit determined by Rietveld refinement. The data indicate that long-range magnetic order is present at 1.27 K, consistent with the magnetic susceptibility results[4] for DyH_3. Extra peaks of magnetic origin are more clearly delineated by the low-angle region of the difference pattern in the Fig. 2 inset, where the nuclear portion of the nuclear+magnetic model fit is subtracted from the 1.27 K powder pattern. At all temperatures measured, good fits, such as the one in Fig. 2, were obtained for the Bragg peaks of nuclear origin with the D_m-disorder $P\bar{3}c1$ model suggested previously for YD_3.[16] No obvious changes in nuclear structure were evident between 1.27 and 295 K. As in the YD_3 study, the D_m-disorder model could be replaced by a perfect-order model in which the elongated D_m scattering density along the *c*-axis direction is taken into account by the addition of a significant anisotropy in the temperature factors for the D_m atoms. In either case, model refinements indicated D/Dy stoichiometric ratios of ~3 within the precision of the fits, which is consistent with the D uptake measurements and places an upper limit of the order of 1% for the *m*-site vacancy fraction. Table I compares the nuclear parameters determined from both model fits with those determined for YD_3.

At 295 K, the perfect-order model yielded the agreement parameters $R_p = 4.02\%$, $R_{wp} = 4.74\%$, and $\chi^2 = 1.023$. Compared with the YD_3 results,[16] the model refinement indicated similar anisotropic behavior in the temperature factors for all of the D atoms. For example, the D_{m1} and D_{m2} atoms exhibited exceptionally large B_{33} values of 16(3) Å^2 and 3.2(4) Å^2, respectively. The data suggested that the D_{m1} temperature factor for DyD_3 was significantly more anisotropic than that for YD_3. The D_t atoms also exhibited somewhat large anisotropic components [$B_{11} = 1.8(2)$ Å^2, $B_{22} = 3.1(3)$ Å^2, and $B_{33} = 2.1(1)$ Å^2], which is suggestive of positional disorder and/or a division of the D_t atoms into more than one type of crystallographic site.

The model fit using the preferred D_m-disorder $P\bar{3}c1$ model yielded good agreement parameters $R_p = 4.05\%$, $R_{wp} = 4.77\%$, and $\chi^2 = 1.036$. The lattice constants at 295 K for the Dy_6D_{18} unit cell were $a = 6.3443(2)$ Å and $c = 6.5983(3)$ Å [$c_0/a_0 = \sqrt{3}c/a = 1.8014(1)$ compared with 1.5732 for Dy metal[28]]. Isotropic temperature factors were 0.93(7) Å^2 for all D_m atoms. Again, there was considerable

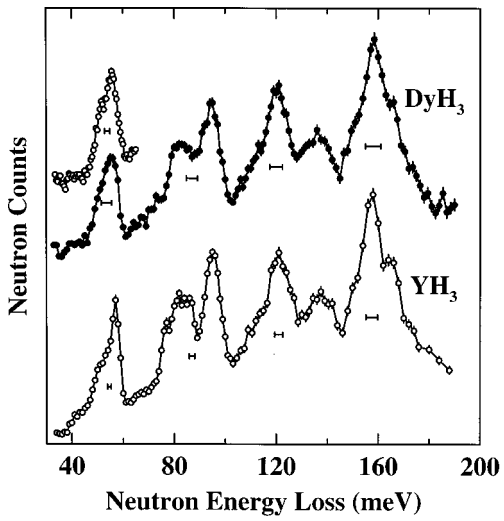

FIG. 3. A comparison of the neutron vibrational spectra for DyH_3 at 17 K and YH_3 at 10 K. Open circles are data collected with the high-resolution filter. The instrumental resolution (FWHM) is depicted by the horizontal bars beneath the spectra.

anisotropy present for the D_t temperature factor [$B_{11}=0.7(3)$ Å^2, $B_{22}=3.9(4)$ Å^2, and $B_{33}=1.7(1)$ Å^2], reflective of the expected positional disorder and/or crystallographic-site division due to the assumed D_m disorder.

Figure 3 compares the neutron vibrational spectrum for DyH_3 at 17 K with the higher-resolution spectrum[29] for YH_3 at 10 K. Advantage was taken of the larger incoherent scattering cross section for H compared to D in this system to help compensate for the attenuation of the scattered beam due to the substantial absorption cross section of Dy. The measured vibrational spectrum for DyD_3 displayed similar isotope-shifted features as DyH_3 but the signal-to-noise ratio was less than satisfactory. The similarity of the H vibrational density-of-states spectra is in line with the NPD results, indicating that the trihydrides of Dy and Y are crystallographically isostructural. As previously pointed out for such a structural arrangement,[25,30] considering the relative geometries and metal-hydrogen bond lengths of the *m* and *t* sites, it is probable that the *c*-axis-polarized vibrations of the H_m atoms account for the lowest-energy vibrational band near 56 meV, and the orthogonal *ab*-plane-polarized vibrations account for the highest-energy vibrational band near 159 meV. Yet, it is clear that any detailed analysis of the entire vibrational spectrum requires more rigorous theoretical calculations.

The data in Fig. 2 reveal additional resolution-limited Bragg peaks that are magnetic in origin, and these are shown more clearly in Fig. 4, where the data at 6 K have been subtracted from the data obtained at 1.27 K. If there is no significant structural distortion associated with the magnetic ordering (as is indicated by the structural refinements), then this subtraction technique eliminates the background and nuclear Bragg peaks, revealing the magnetic diffraction pattern.[31] The strongest magnetic Bragg peak is identified as the (0, 0, 1/2) reflection, which indicates that the basic magnetic structure (see Fig. 5) consists of pairs of ferromagnetic sheets of spins in the *ab* planes that are stacked antiferromagnetically along the *c* axis, with an ordered moment of $5.25(4)\mu_B$.

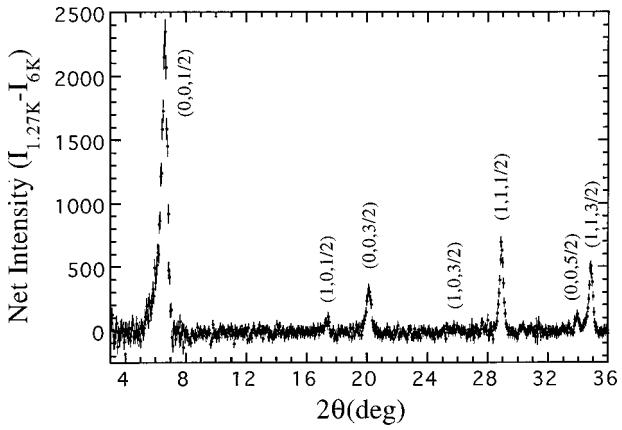

FIG. 4. The magnetic diffraction pattern revealed from BT-1 data by subtraction of the measured pattern at 6 K from that at 1.27 K.

The data of Fig. 4 also indicate weak magnetic peaks at scattering angles near 17° and 26°, which can be indexed as the (1, 0, 1/2) and (1, 0, 3/2) reflections, respectively. These extra reflections were confirmed by BT-2 measurements. For pure ferromagnetic sheets, the intensities of such peaks would be zero, and their observation indicates that a distortion of the basic ferromagnetic model exists in this material. One possibility is that the distortion originates from D-site disorder, which provides a distortion of the local site symmetry of the Dy atoms. A second possibility occurs by noting that the in-plane Dy lattice is triangular. In the case of antiferromagnetic interactions, such a lattice would be fully frustrated, and hence one might expect that an antiferromagnetic distortion might have chiral symmetry.[32] Applying such a

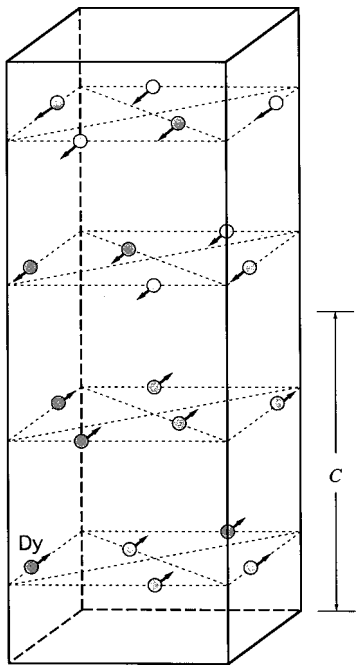

FIG. 5. The basic magnetic structural model of the Dy spin ordering in DyD_3, in which ferromagnetic sheets of spins in the *ab* planes are stacked antiferromagnetically along the *c* axis.

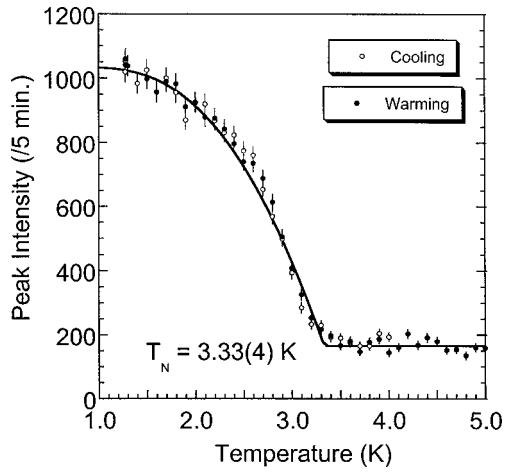

FIG. 6. Temperature dependence of the $(0,0,\frac{1}{2})$ magnetic-ordering peak intensity for DyD_3.

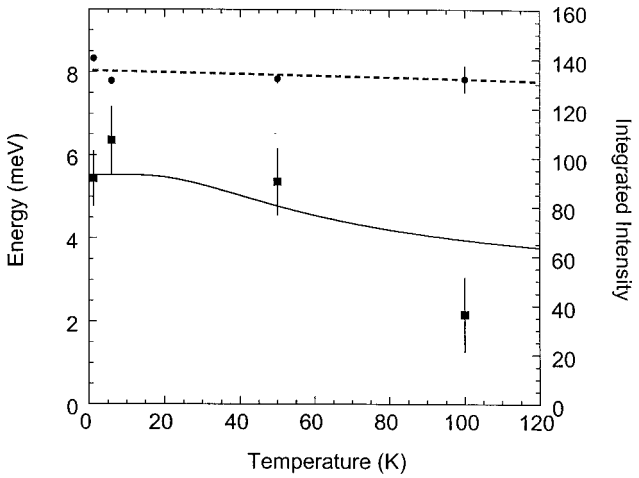

FIG. 8. Temperature dependence of the intensity and energy of the crystal-field excitation for DyD_3.

distortion to the ferromagnetic layer indicates that a relative rotation of each spin by $\sim 10°$ from the parallel configuration would yield the correct intensity for these extra peaks. However, with only two additional peaks, the information that can be obtained is limited, and this model for the distortion should only be considered suggestive. Additional data on single crystals will likely be needed to fully elucidate the ground-state magnetic configuration.

The temperature dependence of the intensity of the (0,0, 1/2) magnetic Bragg peak is shown in Fig. 6. The magnetic intensity is proportional to the square of the sublattice magnetization, and we see that the ordered moment varies smoothly with temperature. There is no evidence of any thermal irreversibilities, and all indications are that the phase transition is second order (i.e., continuous) in nature. The solid curve is a fit to a mean-field model and gives an estimate of the Néel temperature (T_N) of 3.33(4) K.

Inelastic measurements were carried out to search for crystal-field levels of the $J=15/2$ Dy ions, and Fig. 7 shows data at 6 K (which is above the ordering temperature) for a wave-vector transfer of 1.8 $Å^{-1}$. We observe an excitation at 7.79(8) meV, which is a transition from the ground state to an excited crystal-field level. No other excitations from the ground state are observed up to an energy transfer of 25 meV.

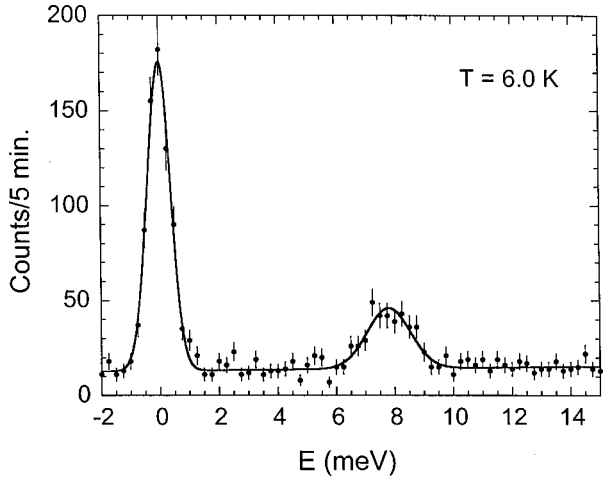

FIG. 7. Inelastic-scattering spectrum of DyD_3 at 6.0 K displaying a crystal-field excitation at 7.79(8) meV.

The intensity of the crystal-field transition is proportional to the population of the initial state (assuming Boltzmann statistics), and a dipole matrix element that couples the initial and final states.[33] Some matrix elements can be quite small, or even zero by symmetry, so that the data of Fig. 7 do not unambiguously identify this excitation as the first excited state. To explore this question, Fig. 8 shows the intensity of this excitation as a function of temperature. The intensity does not vary significantly from low temperature to 50 K, while if there were another unobservable level at an energy substantially lower than 8 meV, then the probability that the Dy ion would be in the crystal-field ground state would decrease, and the intensity should drop. However, we do not observe a significant drop until the 8 meV level (which corresponds to a temperature of ~ 90 K) begins to acquire a significant thermal population, and this indicates that this level is in fact the first excited state. The intensity is then expected to decrease as the ground-state population is depleted, and the solid curve is the calculated variation assuming that both the ground and first excited states are doublets. The error bars represent one standard deviation, and the agreement is reasonable. A somewhat improved fit could be obtained by introducing additional (unresolved) levels at ~ 7.8 meV, effectively increasing the (quasi) degeneracy of the first excited state. However, adding another fitting parameter in the present case is unwarranted in our view, and in any event this does not effect the primary conclusion that only the (doublet) crystal-field ground state is significantly occupied when the system is magnetically ordered. In other words, the higher-energy crystal-field levels do not play a significant role in the magnetic phase transition or spin dynamics of the ordered state. We remark that at 100 K there is already a substantial intrinsic linewidth to the excitation, and this makes it difficult to extend the measurements to higher temperatures.

Finally, Fig. 8 also indicates that there is no significant temperature dependence to the energy over this temperature range, with the exception of a significant shift in the energy below the ordering temperature. Of course, in the ordered state the ions can no longer be considered independent, and

the magnetic excitations will acquire some dispersion as the collective behavior sets in. It would be informative to investigate the spin-wave excitations in the ordered state if single crystals become available.

SUMMARY

The NPD results for DyD_3 and the NVS results for DyH_3 are in accordance with the $P\bar{3}c1$ crystal structure proposed by the earlier YD_3 study. The DyD_3 structural data are well described by a model that assumes D_m positional disorder along the c axis, although a model that assumes perfect D_m positional order with highly anisotropic thermal factors (i.e., large c-axis components) also fits the data. The low-temperature data indicate the onset of antiferromagnetic ordering along the c axis at $T_N = 3.33(4)$ K. The first crystal-field excitation is found at 7.79(8) meV, which implies that the Dy atoms are in their crystal-field ground-state configuration at the ordering temperature.

*Also at Department of Materials and Nuclear Engineering, University of Maryland, College Park, Maryland 20742.

[1] J. N. Huiberts, R. Griessen, J. H. Rector, R. J. Wijngaarden, J. P. Dekker, D. G. de Groot, and N. J. Koeman, Nature (London) **380**, 231 (1996).
[2] R. Griessen, J. N. Huiberts, M. Kremers, A. T. M. van Gogh, N. J. Koeman, J. P. Dekker, and P. H. L. Notten, J. Alloys Compd. **253-254**, 44 (1997).
[3] R. L. Carlin, R. D. Chirico, K. O. Joung, G. K. Shenoy, and D. G. Westlake, Phys. Lett. **75A**, 413 (1980).
[4] R. L. Carlin and L. J. Krause, Chem. Phys. Lett. **82**, 323 (1981).
[5] D. J. Flood, J. Appl. Phys. **49**, 1495 (1978).
[6] P. Vajda, in *Handbook on the Physics and Chemistry of Rare Earths*, edited by K. A. Gschneidner and L. Eyring (Elsevier Science, Amsterdam 1995), Vol. 20, p. 207, and references therein.
[7] T. J. Udovic, Q. Huang, R. W. Erwin, J. W. Lynn, and J. J. Rush (unpublished).
[8] M. Chiheb, J. N. Daou, and P. Vajda, Z. Phys. Chem. (Munich) **179**, 255 (1993).
[9] P. Vajda, G. André, and J. Hammann, Phys. Rev. B **55**, 3028 (1997).
[10] H. Shaked, D. G. Westlake, J. Faber, and M. H. Mueller, Phys. Rev. B **30**, 328 (1984).
[11] J. M. Friedt, G. K. Shenoy, B. D. Dunlap, D. G. Westlake, and A. T. Aldred, Phys. Rev. B **20**, 251 (1979).
[12] G. E. Sturdy and R. N. R. Mulford, J. Am. Chem. Soc. **78**, 1083 (1956).
[13] A. Pebler and W. E. Wallace, J. Phys. Chem. **66**, 148 (1962).
[14] M. Mansmann and W. E. Wallace, J. Phys. (Paris) **25**, 454 (1964).
[15] N. F. Miron, V. I. Shcherbak, V. N. Bykov, and V. A. Levdik, Krystallografiya **17**, 404 (1972) [Sov. Phys. Crystallogr. **17**, 342 (1972)].
[16] T. J. Udovic, Q. Huang, and J. J. Rush, J. Phys. Chem. Solids **57**, 423 (1996).
[17] T. J. Udovic, Q. Huang, and J. J. Rush, Phys. Rev. Lett. **79**, 2920 (1997).
[18] Y. Wang and M. Y. Chou, Phys. Rev. Lett. **71**, 1226 (1993).
[19] Y. Wang and M. Y. Chou, Phys. Rev. B **51**, 7500 (1995).
[20] J. P. Dekker, J. van Ek, A. Lodder, and J. N. Huiberts, J. Phys.: Condens. Matter **5**, 4805 (1993).
[21] P. J. Kelly, J. P. Dekker, and R. Stumpf, Phys. Rev. Lett. **78**, 1315 (1997); **79**, 2921 (1997).
[22] R. Ahuja, B. Johansson, J. M. Wills, and O. Eriksson, Appl. Phys. Lett. **71**, 3498 (1997).
[23] R. Eder, H. F. Pen, and G. A. Sawatzky, Phys. Rev. B **56**, 10 115 (1997).
[24] V. F. Sears, Neutron News **3** (No. 3), 26 (1992).
[25] J. K. Stalick, E. Prince, A. Santoro, I. G. Schroder, and J. J. Rush, in *Neutron Scattering in Materials Science II*, edited by D. A. Neumann, T. P. Russell, and B. J. Wuensch, Mater. Res. Soc. Symp. Proc. No. 376 (Materials Research Society, Pittsburgh, PA, 1995), p. 101.
[26] H. M. Rietveld, J. Appl. Crystallogr. **2**, 65 (1969).
[27] A. C. Larson and R. B. Von Dreele, *General Structure Analysis System* (University of California, Berkeley, 1985).
[28] K. A. Gschneider, Jr., Bull. Alloy Phase Diagrams **11**, 216 (1990).
[29] T. J. Udovic, Q. Huang, and J. J. Rush, in *Hydrogen in Semiconductors and Metals*, edited by N. N. Nickel, W. B. Jackson, R. C. Bowman, and R. G. Leisure, Mater. Res. Soc. Symp. Proc. No. 513 (Materials Research Society, Pittsburgh, PA, 1998), p. 197.
[30] T. J. Udovic, J. J. Rush, Q. Huang, and I. S. Anderson, J. Alloys Compd. **253-254**, 241 (1997).
[31] H. Zhang, J. W. Lynn, W-H. Li, T. W. Clinton, and D. E. Morris, Phys. Rev. B **41**, 11 229 (1990).
[32] For a review, see M. F. Collins and O. A. Petrenko, Can. J. Phys. **75**, 605 (1997).
[33] See, for example, J. W. Lynn, D. E. Moncton, L. Passell, and W. Thomlinson, Phys. Rev. B **21**, 70 (1980).